www.sciencevision.org

Research Note

Sci Vis 12 (1), 11-16
January-March 2012
ISSN (print) 0975-6175
ISSN (online) 2229-6026

Surface state photocurrent calculations in magnetic solids

Lalnunpuia, Aldrin Malsawmtluanga, Z. Pachuau* and R. K. Thapa

Department of Physics, Mizoram University, Aizawl 796 004, India

Received 8 September 2011 | Accepted 12 January 2012

Abstract

Several models have been used for the photoemission calculations from surfaces of magnetic solids like Fe, Ni, Co, Cr and W. We have used the Mathieu potential model which gives a qualitative characteristic of surface state photoemission by considering only the surface contribution from the existing bulk-band structure calculations.

Key words: Photoemission; surface states; Mathieu potential; wave functions; magnetic solids.

PACS No.: 73.20; 79.60

Introduction

In this report, we present the calculations of photocurrent from magnetic solids by using the Mathieu potential to describe the surface regions of solids. Mathieu potential has been used by Levine[1] and Statz[2] for surface state calculations. In this report, we have used the model as described by Davison and Steslicka[3], as shown in Fig. 1. Pachuau *et al.*[4] had applied this model for deriving the initial state wave functions for evaluation of the matrix element $\langle \psi_f | H' | \psi_i \rangle$ to calculate the photocurrent. The photocurrent data as obtained by them in the ultra-violet photon energy range showed interesting features comparable to experimental results[5] especially in the case of tungsten and molybdenum. But the calculation for photocurrent includes those contributions from the bulk region. Hence the calculation in this report shows the variation of photocurrent obtained only by that contribution from the surface region.

Formalism

The photocurrent density formula from Fermi Golden rule approximation used by Penn[6] can be written as

$$\frac{dj(E)}{d\Omega} = \frac{2\pi}{\hbar} \sum |< \psi_f \,|\, \mathrm{H}' \,|\, \psi_i >|^2 \, \delta(E - E_f) \, \delta(E_f - E_i - \hbar\omega) \, f_o(E - \hbar\omega)[1 - f_o(E)] \quad \ldots (1)$$

where $\Psi_i(\Psi_f)$ refer to the initial (final) state wave functions and perturbation H' is given by

$$H' = \frac{e}{2m_e c}\left(\boldsymbol{A.p} + \boldsymbol{p.A}\right) \quad \ldots (2)$$

Corresponding author: Z. Pachuau
Phone: 0389-2330522 Cell: +91 9862770341
E-mail: zpc21@yahoo.com

In Eq. (2), m_e refers to the mass of the electron, $\boldsymbol{p}$ the one-electron momentum operator and $\boldsymbol{A}$ the vector potential of the incident photon field. To compute the photon field, we have used the local dielectric model of Bagchi and Kar[7]. We assume the z-direction to be perpendicular to the surface (which is taken as z = 0 plane), and the surface region is defined by $-d \le z \le 0$ while the metal is assumed to occupy all the space to the left of z=0 plane. Let a *p*-polarised light be incident on the surface plane making an angle θ_i with the z-axis. The vector potential $\tilde{A}_\omega(z)$ in the long wavelength limit $(\frac{\omega d}{c}) \to 0$ is given by

$$\mathring{A}_\omega(z) = \begin{cases} A_1 \quad , & z < -d \quad (bulk) \\ \dfrac{A_1.\varepsilon(\omega).d}{[1-\varepsilon(\omega)]z + d} \ , & -d \le z \le 0 \quad (surface) \\ A_1.\varepsilon(\omega), & z \ge 0. \quad (vacuum) \end{cases} \quad \ldots (3)$$

where A_1 is a constant depending on the dielectric function $\varepsilon(\omega)$, photon energy $\hbar\omega$ and angle of incidence θ_i. Let us consider a one-dimensional crystal whose potential is represented by a sinusoidal potential given by

$$V(x) = V_0 \cos\left(\frac{2\pi x}{a}\right) \quad \ldots (4)$$

where *'a'* is the period of the potential having a maximum value V_0 at x=0. The one-dimensional Schrödinger equation can be written as

$$\frac{d^2\psi(z)}{dz^2} + (\alpha - 2q\cos 2z)\psi(z) = 0 \quad \ldots.. (5)$$

where $2q = \frac{V_0}{a}$, $z = \frac{\pi x}{a}$, $T = \left(\frac{\pi}{a}\right)^2$, $\alpha = \frac{E}{T}$

The surface state will be largely a hybrid of sine and cosine elliptic functions which is given by

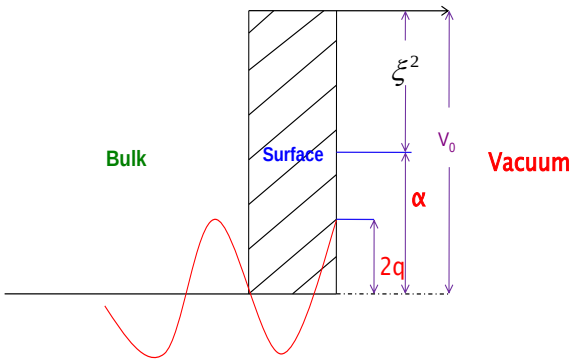

Figure 1. Model diagram of sinusoidal Mathieu Potential used for calculating the initial state wave function.

$$\varphi(x_o^{/}, q) = \lambda_m ce_m(x_o^{/}, q) - se_m(x_o^{/}, q) \quad \ldots (6)$$

where $x_0^{/} = \frac{\pi}{a}.x_0$, x_0 is the location of surface and λ_m is the hybridization parameter which can be written as

$$\lambda_m = \frac{se_m(x'_0, q) - (\xi + \mu)^{-1} se'_m(x'_0, q)}{ce_m(x'_0, q) - (\xi + \mu)^{-1} ce'_m(x'_0, q)} \quad \ldots (7)$$

After expanding the sine and cosine elliptic function, and considering surface state occurring for $m = 3$, we can write

$$ce_3(x'_0, q) = 0 \quad , se'_3(x'_0, q) = 0$$

$$ce'_3(x'_0, q) = 3\left(1 + \frac{q}{16} - \frac{q^2}{640}\right)$$

$$se_3(x'_0, q) = -1 + \frac{q}{16} - \frac{11}{640}q^2 \quad \ldots (8)$$

Hence, we may obtain the value of λ_3 as:

$$\lambda_3 = \frac{(\xi + \mu)\left[1 - \frac{q}{16} + \frac{11}{640}q^2\right]}{3\left(1 + \frac{q}{16} - \frac{q^2}{640}\right)} \quad \ldots (9)$$

Using eqs.(6), (8) and (9), the initial state wave function in the case of strong periodic potential[4] (in atomic units) becomes

$$\psi_i(x,q)=\begin{cases}\left(\frac{1}{4\pi k_i}\right)^{\frac{1}{2}}\left(1-\frac{q}{16}+\frac{11}{640}q^2\right)e^{-\mu(x'_0-x)}, & x\le 0\\ (2\xi)^{\frac{1}{2}}e^{-\xi(x-x'_0)}, & x\ge 0\end{cases} \quad \text{..... (10)}$$

Here, the various constants (in a.u.) used are as follows:

$$q=1,\ k_i^2=2E_i,\ \xi=2,\ x'_0=\frac{\pi}{a}.x_0 \quad \text{... (11)}$$

where a is the lattice constant.

The final state wave function ψ_f used in eq. (1) is the scattering state[9] of the step potential defined by $V(x)=-V_0\theta(x)$, where $\theta(x)$ is unit fraction such that $\theta(x)=1(0)$ *for x>0(x<0)*), which is encountered by the electron and is given by (in atomic units)

$$\psi_f(x)=\left(\frac{1}{2\pi q_f}\right)^{\frac{1}{2}}\frac{2q_f}{q_f+k_f}e^{ik_f x}e^{-\alpha|x|} \qquad x\le 0(\textit{bulk \& surface}) \quad \text{... (12)}$$

where $k_f^2=2E_f$, $q_f^2=2(E_f-V_0)$ and $E_f=E_i+\hbar\omega$.

The factor $e^{-\alpha|x|}$ is included on the bulk and surface side to take into account the inelastic scattering of the electrons.We have calculated photocurrent for locations of the initial state wave functions in the surface region, that is, at x_0.

The matrix element $\langle\psi_f|H'|\psi_i\rangle$ occurring in eq. (1) can be expanded as follows:

$$\mathrm{I}=\langle\psi_f|H'|\psi_i\rangle=\int_{-\infty}^{\infty}\psi_f^*H'\psi_i dz$$

$$=\int_{-\infty}^{\infty}\psi_f^*\left(\tilde{A}_\omega(z)\frac{d}{dz}+\frac{1}{2}\frac{d}{dz}\tilde{A}_\omega(z)\right)\psi_i\, dz$$

$$\mathrm{I}=\int_{-\infty}^{-d}\psi_f^*\,\tilde{A}_\omega\,\psi_i\,dz+\int_{-d}^{0}\psi_f^*\,\tilde{A}_\omega\frac{d\psi_i}{dz}dz$$

$$+\frac{1}{2}\int_{-d}^{0}\psi_f^*\frac{d\tilde{A}_\omega}{dz}\psi_i\,dz+\int_{-d}^{0}\psi_f^*\,\tilde{A}_\omega\,\varepsilon(\omega)\frac{d\psi_i}{dz}dz \quad \text{.... (13)}$$

Considering only the surface contribution, eq. (13) reduces to

$$\mathrm{I}=\int_{-d}^{0}\psi_f^*\tilde{A}_\omega(z).\frac{d\psi_i}{dz}.dz+\frac{1}{2}\int_{-d}^{0}\psi_f^*.\frac{d\tilde{A}_\omega(z)}{dz}.\psi_i.dz \quad \text{... (14)}$$

The above integral cannot be solved analytically. Therefore, FORTRAN program is developed to evaluate these integrals for computing photocurrent as a function of photon energy. Photocurrent was calculated from magnetic solids like Fe, Ni, Co, Cr and W.

RESULTS

We discuss here the results of photocurrent in the case of Fe, Ni, Co, Cr and W. Here we used the experimentally measured dielectric constants as given by Weaver[8] and Edward[9]. Choice of parameter like initial state energy (E_i), state energy (E_i), magnitude of potential (V_0), Fermi level (E_F), were those pertaining to respective magnetic solids. However, angle of incidence was $\theta_i=45^0$ for *p*-polarised light under consideration in all the cases. Photocurrent had been calculated for values of $x_0=-2\ a.u$ and $x_0=-3\ a.u$. As the width of the surface is 10 a.u. in both the cases, $x_0=-2\ a.u$ is near the surface-vacuum interface and $x_0=-3\ a.u$ is towards the surface-bulk interface.

Iron

Fig 2 shows the behaviour of photocurrent in the case of Fe where we have shown the plot for two locations of surface states wave functions, that is, at $x_0=-2\ a.u$ and $x_0=-3\ a.u$. The

observed value of plasmon energy ($\hbar\omega_p$) of Fe[10] is 15.8 eV. In the case of wave function located at $x_0 = -2\ a.u$ plot of photocurrent showed a maxima at $\hbar\omega = 9$ eV and it is decreased to a minima at $\hbar\omega = 13$ eV. A second peak of small magnitude in height was found at $\hbar\omega = 15$ eV. The case of $x_0 = -3\ a.u$ shows a different trend which decreases rapidly as the photon energy increases and also having a minima at $\hbar\omega = 13$ eV. However, we have not observed proper peak in photocurrent near plasmon energy of iron.

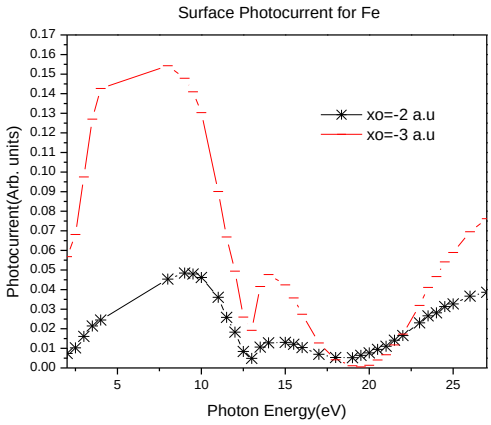

Figure 2. Plot of photocurrent against the photon energy (eV) for Fe.

Nickel

Fig 3 shows the behaviour of photocurrent in the case of Ni where we have shown the plot again for two locations of surface states wave functions, that is, at $x_0 = -2\ a.u$ and $x_0 = -3\ a.u$. The observed value of surface plasmon energy ($\hbar\omega_p$) of Ni[11] is 16.2 eV. In the case of wave function located at x_0 = -2 $a.u$ plot of photocurrent showed a maxima at $\hbar\omega = 9$ eV and it is decreased to a minima at $\hbar\omega = 13$ eV. A second peak of small magnitude in height was found at $\hbar\omega = 14$ eV. The case of $x_0 = -3\ a.u$ shows a different trend which decreases rapidly as the photon energy increases and having a minima also at $\hbar\omega = 13$ eV.

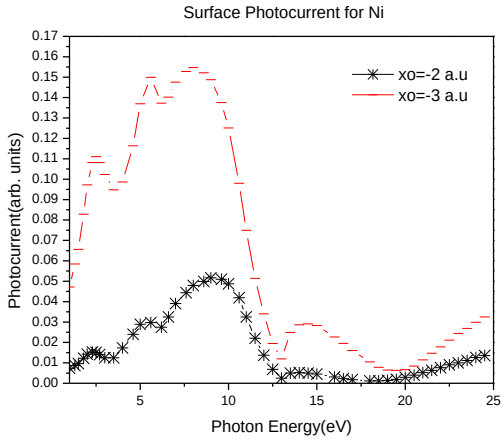

Figure 3. Plot of photocurrent against the photon energy (eV) for Ni.

Cobalt

Fig 4 shows the behaviour of photocurrent in the case of Co where we have shown the plot for two locations of surface states wave functions, that is, at $x_0 = -2\ a.u$ and $x_0 = -3\ a.u$. In the case of wave function located at $x_0 = -2\ a.u$ plot of photocurrent showed a maxima at $\hbar\omega = 7.7$ eV and it is decreased to a minima at $\hbar\omega =$ 15.5 eV. The case of $x_0 = -3\ a.u$ shows a different trend which decreases rapidly as the photon energy increases and having a minima also at $\hbar\omega = 12.4$ eV.

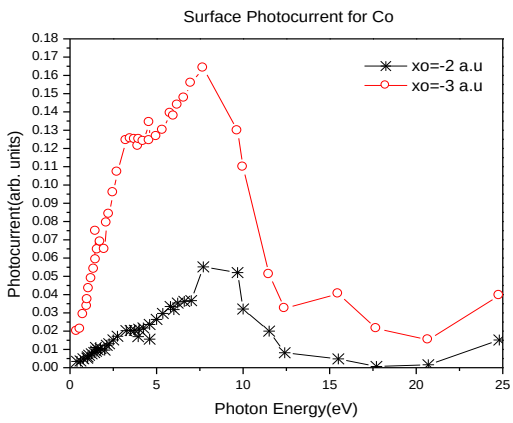

Figure 4. Plot of photocurrent against the photon energy (eV) for Co.

Chromium

Fig 5 shows the behaviour of photocurrent in the case of Cr where we have shown the plot again for two locations of surface states wave functions, that is, at $x_0 = -2\ a.u$ and $x_0 = -3\ a.u$. In the case of wave function located at $x_0 = -2\ a.u$ plot of photocurrent showed a maxima at $\hbar\omega =$ 4.5 eV and it decreased to a minima at $\hbar\omega =$ 7 eV. A second peak of larger magnitude in height was found at $\hbar\omega =$ 9 eV. The case of $x_0 = -3\ a.u$ shows a different trend showing nearly equal peaks at 4.5 eV and 8.5 eV which decreases rapidly as the photon energy increases and having a minima also at $\hbar\omega =$ 7.5 and 13 eV.

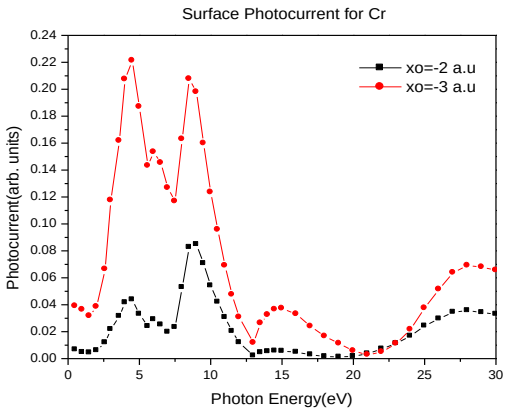

Figure 5. Plot of photocurrent against the photon energy (eV) for Cr.

Tungsten

Fig 6 shows the behaviour of photocurrent in the case of W where we have shown the plot again for two locations of surface states wave functions, that is, at $x_0 = -2\ a.u$ and $x_0 = -3\ a.u$. The observed value of plasmon energy ($\hbar\omega_p$) of W[11,12] is 23 eV. In the case of wave function located at $x_0 = -2\ a.u$ plot of photocurrent showed a maxima at $\hbar\omega =$ 7.5 eV and it decreased to a minima at $\hbar\omega =$ 12.8 eV. No significant second peak was found. The case of $x_0 = -3\ a.u$ shows a similar trend which decreases rapidly as the photon energy increases and having a minima also at $\hbar\omega =$ 12.8 eV. A second peak was found in this case having maximum (minimum) at 19.2 eV(23.5 eV).

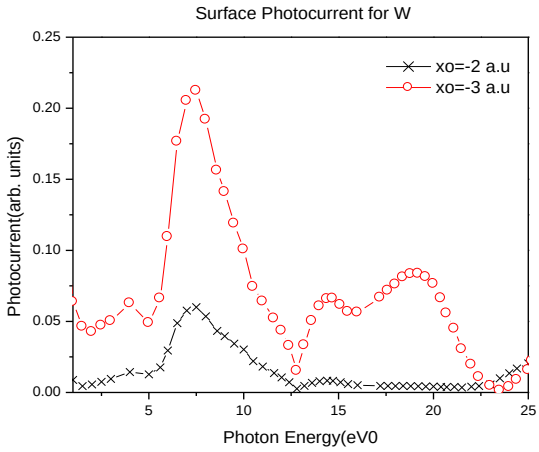

Figure 6. Plot of photocurrent against the photon energy (eV) for W.

DISCUSSIONS AND CONCLUSION

We find that in case of magnetic solids discussed, photocurrent showed almost similar trend. For example in the case of Fe, as photon energy increased, photocurrent reached a maximum at around the values of photon energy equal to plasmon energy of metals. Beyond the plasmon energy, a second peak in photocurrent was obtained whose height is smaller in magnitude than the first one at $\hbar\omega < \hbar\omega_p$. The reason for the occurrence of peak in photocurrent at $\hbar\omega < \hbar\omega_p$ is due to surface refraction effect where the z-component of electromagnetic field becomes maximum at $\hbar\omega = \hbar\omega_p / \sqrt{2}$. This had been also seen in the experimental[5] results of W and Mo. A study of these cases shows one can use Mathieu potential

model for photocurrent calculations especially for surface region of magnetic metals.

References

1. Levine JD (1968). Ionic, covalent, and surface states of a one-dimensional Mathieu potential with arbitrary termination. *Phys Rev*, **171**, 701.
2. Statz H (1950). *Z Naturforsch*, ***5A***, 534.
3. Davison SG & Levine JD (1970). *Solid State Physics.* Academic Press, New York and London, Vol. 25.
4. Pachuau Z, Zoliana B, Khathing DT, Patra PK & Thapa RK (2002). Application of Mathieu Potential to photoemission calculations: the case of a strong potential. *Phys Lett*, ***A* 294**, 52.
5. Weng SL, Gustaffson T & Plummer EW (1978). Experimental and theoretical study of the surface resonances on the (100) faces of W and Mo. *Phys Rev*, **B18**, 1718.
6. Penn DR (1972). Photoemission spectroscopy in the presence of adsorbate-covered surfaces. *Phys Rev Lett*, **28**, 1041.
7. Bagchi A & Kar N (1978). Refraction effects in angle-resolved photoemission from surface states on metals. *Phys Rev*, ***B*18**, 5240.
8. Weaver JH (1987). *Handbook of Chemistry and Physics.* CRC Press, Boca Raton, FL.
9. Pallick ED (ed.) (1991). *Handbook of Optical Constants of Solids.* Academic Press.
10. Glicksman M (1971). Plasmas in solids. *Solid State Phys,* **26**, 338.
11. Moneta M & Pawowski B (2005). Ion stopping cross-section at ferro-paramagnetic phase transition. *Vacuum*, **78**, 467-472.
12. Egelhoff Jr. WF, Linnett JW & Perry DL (1976). Photoemission from surface state of W(100): Evidence for $\vec{p}\cdot\vec{A}$ mode of photoionization. *Phys Rev Lett*, **36**, 98-100.

